Food Chemistry: X 26 (2025) 102306

Contents lists available at ScienceDirect

Food Chemistry: X

journal homepage: www.sciencedirect.com/journal/food-chemistry-x

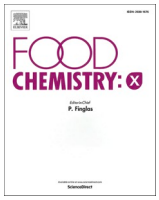

Insight into the effect of wheatgrass powder on steamed bread properties: Impacts on gluten polymerization and starch gelatinization behavior

Muhammad Bilal [b], Yiwei Wu [b], Guangzheng Wang [b], Guannan Liu [b], Muhammad Shahar Yar [b], Dandan Li [a,b], Chong Xie [a,b], Runqiang Yang [a,b], Dong Jiang [a,c], Pei Wang [a,b,*]

[a] The Sanya Institute of Nanjing Agricultural University, Sanya 572024, PR China
[b] College of Food Science and Technology, Whole Grain Food Engineering Research Center, Nanjing Agricultural University, Nanjing, Jiangsu 210095, PR China
[c] National Technique Innovation Center for Regional Wheat Production/Key Laboratory of Crop Physiology, Ecology, and Management, Ministry of Agriculture/National Engineering and Technology Center for Information Agriculture, Nanjing Agricultural University, Nanjing, Jiangsu 210095, PR China

ARTICLE INFO

Keywords:
Wheat seedlings
Bioactive compounds
Functional food additive
Techno-functionality
Gluten proteins
Starch gelatinization

ABSTRACT

This study investigates the use of wheatgrass powder (WGP) as a functional ingredient in steamed bread, focusing on its effects on the nutritional composition and key biological macromolecules, specifically gluten and starch. Wheatgrass harvested at 8 days demonstrated optimal bioactive content, enhancing steamed bread quality. The incorporation of WGP (2.5 % and 5 %) reduced loaf volume and increased firmness and chewiness while improving flavor and taste. WGP also suppressed starch gelatinization, decreased thermal stability, and altered gluten polymerization by reducing the polymerization of α- and γ-gliadin into glutenin. Scanning electron microscopy (SEM) analysis revealed that WGP disrupted the gluten-starch matrix, leading to a fragmented gluten network and reduced starch gelatinization, which contributed to the increased firmness and chewiness of steamed bread. These findings highlight the potential of WGP as a functional ingredient for wheat-based products and fill the gap by providing WGP insights into the optimization of dough properties and the underlying molecular interactions involving proteins and starch.

1. Introduction

Germination and sprouting processes are recognized for enhancing bioactive compounds, including folates, and γ-aminobutyric acid (GABA), phenolic compounds, particularly under carefully managed germination parameters (Kaur et al., 2021; Liu, Zhou, et al., 2024). Wheatgrass, a member of the *Gramineae* (*Poaceae*) family, is increasingly recognized for its potential as a nutritional supplement with numerous health benefits. The functional properties of wheat seedlings are associated with their diverse dietary composition, which comprises essential vitamins (A, B, C, and E), along with minerals, flavonoids, phenolic compounds, amino acids, and chlorophyll (Ghumman et al., 2017; Kaur et al., 2021). The fortification of food products with wheatgrass can be regarded as a scientifically advanced, procedurally viable, and practically feasible approach to augmenting the dietary intake of bioactive compounds.

Steamed bread is a fundamental dietary staple food in China, consumed by most of the population and contributing to approximately 40 % of the national total wheat intake (Bilal et al., 2023). Steamed bread made from refined wheat flour typically exhibits a limited nutritional composition, primarily consisting of starch and gluten proteins (Parenti et al., 2020). Globalization and urbanization have led to significant lifestyle changes among consumers, resulting in a growing demand for health-oriented and convenient food products. Integrating plant-derived ingredients into steamed bread is anticipated to enhance its nutritional profile. Prior research indicates that adding WGP can significantly improve the nutritional profile and sensory qualities of wheat-derived food products. For instance, including WGP in muffin batter has increased viscosity, hardness, and total phenolic content in the final baked muffins (Rahman et al., 2015). Similarly, higher levels of WGP improve the protein, fiber, and antioxidant activities of functional pasta (Bawa et al., 2022). However, a drawback of incorporating WGP in wheat-based products is the deteriorated techno-functionality of dough, which can significantly reduce the organoleptic properties of the product. The techno-functionality of dough is mainly determined by the gluten proteins and starch properties during the processing (Bilal et al., 2024; Wang et al., 2023). With increasing temperature during heating, gluten undergoes disulfide bond-mediated polymerization, leading to

* Corresponding author at: The Sanya Institute of Nanjing Agricultural University, Sanya 572024, PR China.
E-mail address: wangpei@njau.edu.cn (P. Wang).

https://doi.org/10.1016/j.fochx.2025.102306
Received 15 November 2024; Received in revised form 25 January 2025; Accepted 18 February 2025
Available online 21 February 2025

the formation of stable gluten networks. This heat-induced structural development is essential for determining the final loaf volume and texture characteristics of the product. Additionally, starch gelatinization greatly influenced the textural characteristics of wheat products, influencing characteristics such as firmness and elasticity (Wang et al., 2021). Currently, there is a lack of theoretical research examining the effect of WGP on the quality of steamed bread as well as the techno-functionality of dough from the dynamic changes of gluten proteins and starch during processing.

Against this background, the present study aims to assess the nutritional and techno-functional properties of wheat seedlings harvested at different periods. The optimal WGP was selected through the comprehensive analysis of bioactive compounds and their effect on the steamed bread quality. The gluten proteins and starch properties during the dough processing stage have been evaluated to interpret the underlying mechanism of dough techno-functionality. This research can potentially encourage the exploitation of WGP as an innovative functional ingredient in wheat-based products and promote the development of healthy staple foods.

2. Materials and methods

2.1. Materials

The Jimai 22 variety of wheat (*Triticum aestivum*) was cultivated and harvested in 2022 by the College of Agriculture at Nanjing Agricultural University in Jiangsu Province, China. This variety was selected based on its high grain quality and its suitability for the intended experimental conditions. Active dry yeast, sourced from Angel (Hubei, China) and common wheat flour, was obtained from a local supermarket in Nanjing. Purified water was produced using a Millipore purification system (Waters, Mississauga, Ontario, Canada). All reagents utilized in the study were of analytical grade unless otherwise noted.

2.2. Cultivation of wheat seedlings

Wheat seedlings were grown by planting the wheat seeds according to the method of Rahman et al. (2015) with slight modifications. Wheat seeds were weighed and washed with pure water to remove contamination. A plastic tray covered with moist muslin cloth and seeds with calculated weight was added onto the tray, and the tray was again covered with wet muslin cloth to assist germination. After two days, the cloth was removed, and the seedlings were harvested on different germination days.

2.3. Preparation of wheatgrass powder (WGP) and its approximate composition

After harvesting, the height and fresh and dried weight of wheat seedlings were determined. The dried wheatgrass was processed into a fine powder using an ultra-centrifugal mill (ZM 200, Retsch, Germany). This powder was then passed through a 60-mesh sieve to ensure a consistent particle size and was subsequently kept at −80 °C for future analyses. The compositional analysis of the wheatgrass powder (WGP) was conducted following established International Approved Methods, moisture (AACC 44–16.01), protein (AACC 39–25.01), fat (AACC 58–19.01), ash content (AACC 08–01.01), and total dietary fiber (AACC 32–05.01) as outlined by the American Association of Cereal Chemists (International, 2000).

2.4. Determination of total phenols, total flavonoids content, and antioxidant activity of wheatgrass powder (WGP)

One gram of the WGP was extracted with 80 % methanol three times (10 mL each time), then centrifuged at 10000 rpm at 4 °C for 15 min. After centrifugation, the extracts are combined and filtered.

2.4.1. Determination of total phenolic content

Total phenolic content was measured by the prescribed method with slight modifications (Kaur et al., 2021). Briefly, 0.5 mL of the sample extract was mixed with 2.5 mL of 10 % aqueous Folin-Ciocalteu reagent and 2.5 mL of 7.5 % sodium carbonate (Na_2CO_3) solution. The resulting mixture was thoroughly vortexed and incubated in the dark at ambient temperature for 2 h. After incubation, absorbance was recorded at 765 nm using a UV–visible spectrophotometer to quantify the phenolic compounds.

2.4.2. Determination of total flavonoid content

Total flavonoid content was determined using a modified aluminium chloride assay method as described by Li, Liu, et al. (2023) with some modifications. Specifically, 300 μL of the extract was mixed with 1.25 mL of deionized water and 100 μL of a 5 % sodium nitrite solution. Following a 6-min incubation, 150 μL of a 10 % aluminium chloride hydrate solution was introduced, allowing the reaction to proceed for 5–10 min. Subsequently, 500 μL of 1 M sodium hydroxide solution and 300 μL of ethanol were added. The final volume was adjusted to 2.5 mL with deionized water, and the absorbance was measured at 510 nm using a UV–Vis spectrophotometer.

2.4.3. Determination of antioxidant properties in-vitro

2.4.3.1. DPPH-free radical scavenging ability. Take 200 μL of the above extracted solution and add 3.8 mL of DPPH solution, vortex, and place in the dark at room temperature for 1 h to react, and measure the absorbance value A at 515 nm.

2.4.3.2. ABTS-free radical scavenging ability. Take 100 μL of the above extraction solution and add 3.0 mL ABTS solution, vortex, and place in the dark at room temperature for 30 min to react, and measure the absorbance value A at 734 nm (Dudonne et al., 2009).

2.5. Nutritional analysis in wheatgrass powder (WGP)

2.5.1. Determination of GABA content

To determine the GABA content, 1 g of the sample was extracted with 5 mL of 7 % (*v*/v) acetic acid solution. The mixture was centrifuged at 20,000 ×*g* for 20 min, and the supernatant was subsequently combined with 5 mL of ethanol and stored at 4 °C for 12 h to allow for sedimentation. Afterwards, the mixture underwent a second centrifugation under identical conditions to eliminate residual acetic acid and ethanol. The resulting pellet was dissolved in 1 mL of 1 M $NaHCO_3$ (pH 9) and centrifuged again at 10,000 ×*g* for 10 min. The final supernatant was treated with 1 mL of dabsyl chloride (4 mg/mL in acetone), incubated at 67 °C for 10 min, and then quenched on ice. The absorbance was measured at 425 nm, and GABA concentration was quantified using a high-performance liquid chromatography (HPLC) system (Agilent 1200 Series, Agilent Technologies, Santa Clara, CA, USA) equipped with a ZORBAX Eclipse AAA reversed-phase column.

2.5.2. Determination of folates content

The total folate content was quantified using high-performance liquid chromatography and mass spectrometry (HPLC-MS). For the extraction, 0.1 g of the sample was homogenized with 10 mL of a buffer solution and subjected to boiling for 10 min. After allowing the mixture to cool at room temperature for 10 min, 150 μL of rat serum was introduced, followed by incubation at 37 °C for 4 h. The sample was then reheated for another 10 min, cooled, and centrifuged at 8000 rpm for 5 min. The supernatant obtained was filtered through a 0.45 μm membrane for purification. Chromatographic analysis was carried out using a C18 column, maintaining a flow rate of 1 mL/min, an injection volume of 20 μL, and a column temperature of 30 °C. The mobile phase employed a 0.05 M potassium dihydrogen phosphate buffer (Phase A)

and acetonitrile (Phase B), as modified from the method described by Riaz et al. (2019).

2.5.3. Determination of chlorophyll content

The total chlorophyll content (TCC) of WGP was estimated using the method of Hiscox and Israelstam (1979). Chlorophyll a and b content was using the following equations:

Chlorophyll a (mg/g) = [(12.7 × A_{663}) - (2.69 × A_{645})] × ml DMSO/mg sample.

Chlorophyll b (mg/g) = [(22.9 × A_{645}) - (4.68 × A_{663})] × ml DMSO/mg sample.

Where A_{663} and A_{645} are the absorbance values at 663 and 645 nm, respectively.

To determine the total chlorophyll content in the WGP, chlorophyll *a* and b values were added together.

2.6. Preparation of steamed bread

The control group consisted of a basic formulation using common wheat flour, dry yeast, and water, the quantity of which was determined by farinograph analysis. The optimum dosage of WGP was 2.5 % and 5 % according to the preliminary study considering the sensory quality of steamed bread fortified with WGP and was referred to as 2.5 %-wheatgrass steamed bread (2.5 %-WGSB) and 5 %-wheatgrass steamed bread (5 %-WGSB). All ingredients were thoroughly blended and kneaded using a planetary mixer (C-100 Mixer, Hobart Corporation, Ohio, USA) at a speed range of 60–120 rpm for 4–6 min to ensure complete dough development. The mixing time was meticulously adjusted based on initial trials to obtain a uniform dough with the desired steamed bread characteristics. The dough was then proofed in a proofing chamber (Model JXFD 7, Dongfu Jiuheng Instrument Technology Co. Ltd., Beijing, China) at 35 ± 2 °C with 75 ± 5 % relative humidity until optimal fermentation height was reached. After fermentation, the dough was steamed over water for 20–25 min. After steaming, the bread was cooled at ambient temperature for 2 h, and quality assessments were conducted within 12 h of preparation (Wang, Liu, et al., 2019).

2.7. Quality analysis of steamed bread

The quality assessment of steamed bread was carried out following the methodology described by Huang et al. (1993), with minor adjustments to suit the specific conditions of this study. The loaf volume was determined using the millet seed displacement technique, a standard method for volume measurement. The spread ratio was evaluated using a vernier caliper by calculating the ratio of the bread's width to its height. A CR-300 chroma meter was employed to assess the crust and crumb color. For texture analysis, a CT3 texture analyzer (Ametek-Brookfield Ltd., USA) fitted with a 40-mm cylindrical acrylic probe was used. Steamed bread samples were cut into uniform slices, each 25 mm thick. These slices were subjected to a compression test at a speed of 1.0 mm/s, compressing them to 50 % of their original thickness, with a 5-s interval between consecutive compressions.

2.8. Analysis of flavor and taste profiles

2.8.1. Electronic nose analysis

The volatile flavor compounds of the steamed bread samples were assessed using a PEN3 electronic nose (e-nose) system (Airsense, Germany) equipped with an array of 10 metal oxide sensors. For the analysis, 1.0 g of each sample was placed into a 15 mL vial, and a static headspace was generated. The vials were sealed and maintained at 60 °C for 20 min to allow the volatiles to equilibrate. After this equilibration period, air, serving as the carrier gas, was introduced into the sensor chamber at a flow rate of 300 mL/min at ambient temperature. Headspace volatiles were measured while the system was sealed, with the sensors undergoing a 180 s cleaning cycle followed by a 60 s sampling period.

2.8.2. Electronic tongue analysis

The taste profiles of steamed bread samples were assessed using the Astree electronic tongue (e-tongue) (Alpha M.O·S, France), equipped with an automated sampling unit and a range of chemical sensors. For each sample, 4 g of steamed bread was soaked in 50 mL of ultrapure water, followed by extraction and equilibration at 60 °C for 20 min. The resulting mixture was centrifuged at 12,000 ×*g* for 10 min. A 30 mL aliquot of the supernatant was diluted to a final volume of 100 mL using ultrapure water, forming the test solution. The test solution was placed into a 100 mL beaker for analysis, with measurements alternating between the ultrapure water and the test solution, and each analysis cycle lasted 120 s (Liu et al., 2023).

2.9. Rapid visco analyzer (RVA)

Four grams of the sample (adjusted to 14 % moisture content) were combined with 25 mL of distilled water in a sample container and mixed thoroughly using a mechanical mixer. The testing protocol commenced by equilibrating the flour suspension at 50 °C for 1 min, with constant stirring at 160 rpm. The temperature was then progressively raised to 95 °C at a rate of 7.5 °C per minute and maintained for 5 min at 95 °C. Subsequently, the temperature was lowered back to 50 °C at a rate of 5 °C per minute and stabilized at 50 °C for 2 min (Wang, Liu, et al., 2019).

2.10. Characteristics of gluten proteins

2.10.1. Molecular weight (Mw) distribution of proteins

Size-exclusion high-performance liquid chromatography (SE-HPLC) was performed using an Agilent 1200 Series HPLC system (Agilent Technologies, Santa Clara, CA, USA) according to Wang et al. (2018) with some modifications. In detail, freeze-dried samples (40 mg) were suspended in 4 mL of 0.05 M sodium phosphate buffer (pH 6.8) containing 2.0 % sodium dodecyl sulfate (SDS) to extract soluble proteins. The mixture was stirred at room temperature for 1 h. Reduced samples were prepared using the same SDS buffer with the addition of 1.0 % dithiothreitol (DTT). After centrifugation at 10,000 ×*g* for 10 min, 20 μL of the supernatant was injected into a Shodex Protein KW-804 column (Showa Denko, Kyoto, Japan). Proteins were eluted with 0.05 M sodium phosphate buffer (pH 6.8) containing 0.2 % SDS at a flow rate of 0.7 mL/min, with the column maintained at 30 °C. Detection was performed at a wavelength of 214 nm. Protein extractions were conducted in triplicate. The areas corresponding to SDS-soluble polymers (SDS-P), monomers (SDS-M), and insoluble proteins (SDS-I) were calculated based on their normalized peak areas.

2.10.2. Determination of free sulfhydryl (SH) groups

The total free sulfhydryl (SH) content was quantified following a modified version of the method described by Beveridge et al. (1974). A sample weighing 40 mg was mixed with 4 mL of a reaction buffer composed of 86 mM Tris, 92 mM glycine, 4.1 mM EDTA [Tris-glycine-EDTA (TGE)], and 2.5 % SDS, adjusted to a pH of 8.0. The mixture was incubated at 25 °C for 30 min, with gentle stirring at 10-min intervals. After incubation, 40 μL of Ellman's reagent [5,5-dithiobis-2-nitrobenzoic acid (DTNB) in TGE (4 mg/mL)] was introduced. The tubes were then shielded from light by wrapping in aluminium foil and incubated for more 30 min at 25 °C. The absorbance of the supernatant was recorded at 412 nm using a blank control that contained no sample or Ellman's reagent.

2.10.3. Distribution of different protein subunits

Lyophilized samples (500 mg) were dissolved in 3 mL of 60 % ethanol and stirred at room temperature (20 °C) for 20 min. The mixture was then centrifuged at 10,000 ×*g* for 10 min at 20 °C, and this

extraction process was performed three times. The resulting supernatants were pooled and diluted with 60 % ethanol to a final volume of 8 mL. Subsequently, the precipitated material underwent further extraction using a buffer solution containing 50 % n-propyl alcohol, 0.05 M Tris-HCl (pH 7.5), 2 M urea, and 1 % DTT, with three additional extraction cycles using 3 mL of buffer each time. The collected supernatants from this step were combined and adjusted to a total volume of 9 mL. For protein separation, 20 µL of the extract was injected into a Nucleosil 300–5 C8 column (Machery-Nagel, Düren, Germany). The chromatographic separation was carried out using deionized water (A) and acetonitrile (B), both containing 0.1 % (*v*/v) trifluoroacetic acid. Proteins were eluted using a linear gradient ranging from 24 % to 56 % solvent B over 50 min at a flow rate of 1.0 mL/min, with detection at 214 nm.

2.11. Analysis of the microstructure of dough

Scanning electron microscopy (SEM) was performed to determine the effects of WGP on the gluten network (Li et al., 2021). The dough samples underwent freeze-drying, followed by fracturing and gold sputtering for 2 min. The microstructural analysis was performed using a Microtrac Semtrac Mini (Nikkiso, Tokyo, Japan) scanning electron microscope, operated at an accelerating voltage of 3.00 kV.

2.12. Statistical analysis

The results are expressed as mean ± standard deviation (SD) based on a minimum of three independent replicates. Data analysis was carried out using SPSS version 19.0 and Origin version 8.6. Statistical significance was assessed through one-way analysis of variance (ANOVA), and differences were considered statistically significant at $p < 0.05$.

3. Results and discussion

3.1. Effect of germination time on the bioactive components and proximate composition in wheat seedlings

The developmental stages of wheat seedlings are depicted in Fig. 1 A, illustrating the progression from seeds to sprouts and, ultimately to seedlings. As germination time was extended, the hypocotyls of the wheat extended, giving rise to fully grown seedlings. Significant physiological changes were observed in the wheat seedlings at various stages

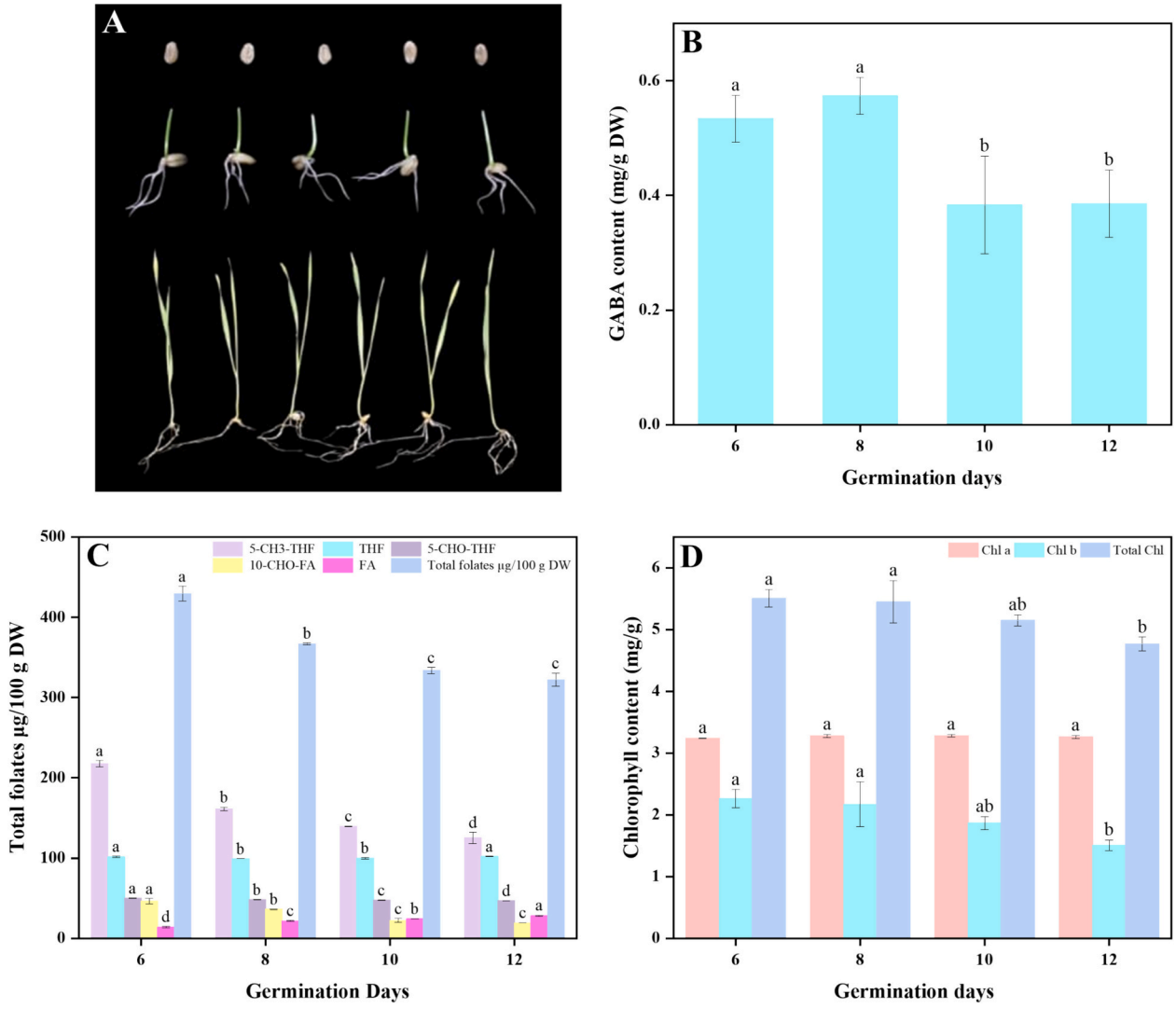

Fig. 1. Images depicting the developmental stages of wheat seedlings illustrate the progression from seeds to sprouts and, ultimately to seedlings germinated under controlled conditions (1 A). Distribution of GABA (1 B), Total Folates (1C), and TCC contents (1 D) in wheat seedlings across different germination periods. GABA, Gamma-aminobutyric acid; THF, tetrahydrofolate; FA, folic acid; 10-CHO-FA, 10-formyl-FA; 5-CHO-THF, 5-formyl-THF; 5-CH3-THF, 5-methyl-THF; TCC, Total chlorophyll content. Different lowercase letters indicate significant differences in germination days ($p < 0.05$).

of germination. Notably, seedling height and dried weight substantially increased with the progressed germination time (Table 1). The protein content and total dietary fiber also exhibited a notable increase during the growth of wheat seedlings. The high dietary fiber and protein content contributes to the nutritional profile of wheat seedlings, making them a valuable ingredient in the functional food recipe. The total phenolic contents of wheat seedlings showed no statistically significant variations across all samples. However, a discernible decrease in total flavonoid content was noted during the growth of wheat seedlings. The flavonoid content during germination is linked to the biochemical processes occurring in seeds, potentially leading to the biosynthesis of secondary plant metabolites such as anthocyanins and flavonoids (Xu et al., 2017). The DPPH assay revealed a substantial decrease in radical scavenging activity with longer germination periods, suggesting a possible reduction in certain antioxidant compounds. Some vitamins, phenolic, and flavonoid compounds were synthesized in wheat seedlings during the initial phases of germination, thereby achieving peak antioxidant capacity after 6–8 days of plant growth (Devi et al., 2019).

The evolution of gamma-aminobutyric acid (GABA) content in wheat seedlings exhibited statistically significant differences across various germination days (Fig. 1 B). Wheat seedlings on the 6 and 8 d of germination exhibited the highest GABA content (~0.55 mg/g DW). This variation in GABA content across different germination stages could be attributed to the dynamic changes in the biochemical and physiological processes occurring during seed germination. The observed increment in GABA content during the initial phases of germination (6 and 8 d) might be associated with the stimulation of glutamate decarboxylase (GAD) enzyme, which triggers the switching of glutamate to GABA (Nonogaki et al., 2010). Additionally, the depletion of stored proteins and carbohydrates in the seed during germination could increase free amino acids, including glutamate, which serves as a precursor for GABA synthesis (Nonogaki et al., 2010). A progressive decline in folate content was observed with increasing germination time (Fig. 1 C), with measurements of 429.46 μg/100 g DW, 366.81 μg/100 g DW, 333.54 μg/100 g DW, and 322.09 μg/100 g DW on the 6, 8, 10, and 12 d, respectively. LC-MS/MS analysis revealed that tetrahydrofolate (THF), 5-methyltetrahydrofolate (5-CH_3-THF), and 5-formyltetrahydrofolate (5-CHO-THF) comprised 90 % of the total folates at different germination stages, indicating these were the predominant folate derivatives in wheat seedlings. The accumulated folate content might be attributed to the quick formation of folate driven by the heightened demand for methyl groups (1C units) during germination (Liu et al., 2017). After seed germination, the endogenous proteases were triggered, leading to the hydrolysis of stored proteins and an incremental rise in peptides and free amino acids. Since glutamic acid is a substrate in folate synthesis, its increase can directly enhance folate production (Ma et al., 2018). In the later phases of germination, the depletion of nutrients in the endosperm, decline in plant vitality, and reduction in metabolic activity lead to a decreased demand for 1C units, subsequently resulting in reduced folate synthesis in wheat seedlings (Lee et al., 2021). With increasing germination days, the chlorophyll *b* of wheat seedlings decreased significantly, resulting in reduced total chlorophyll content after 8 d (Fig. 1 D). Variations in chlorophyll content may arise from environmental stressors and differences in light intensity during plant development (Sani et al., 2024). Overall, 6 and 8 d germinated wheat seedlings exhibited higher nutritional and bioactive properties as compared to other germination days.

Table 1
Physiological development of wheat seedlings from germination to harvest and the analysis of bioactive compounds across different germination periods.

Parameters	6-DWGP	8-DWGP	10-DWGP	12-DWGP
Physiological parameters				
Seedlings Height (cm)	9.43 ± 1.12^{d}	12.63 ± 0.97^{c}	14.56 ± 1.06^{b}	16.63 ± 0.85^{a}
Fresh Seedlings Weight (g)	0.80 ± 0.01^{d}	1.12 ± 0.02^{c}	1.35 ± 0.03^{b}	1.85 ± 0.02^{a}
Dried Seedlings Weight (g)	0.18 ± 0.02^{d}	0.24 ± 0.02^{c}	0.27 ± 0.01^{b}	0.29 ± 0.01^{a}
Proximate components				
Moisture (%)	7.20 ± 0.29^{a}	7.00 ± 0.21^{a}	7.26 ± 0.37^{a}	6.83 ± 0.31^{a}
Protein (%)	23.30 ± 0.34^{d}	26.33 ± 0.13^{c}	27.40 ± 0.21^{b}	28.48 ± 0.10^{a}
Fat (%)	0.21 ± 0.01^{a}	0.20 ± 0.02^{a}	0.20 ± 0.02^{a}	0.18 ± 0.02^{a}
Ash (%)	2.5 ± 0.15^{a}	2.6 ± 0.15^{a}	2.7 ± 0.21^{a}	2.5 ± 0.40^{a}
Total Dietary Fiber (%)	36.19 ± 0.44^{d}	37.44 ± 0.31^{c}	39.85 ± 0.32^{b}	43.61 ± 0.35^{a}
Bioactive and antioxidant indices				
TPC (mgGAE/g DW)	5.47 ± 0.40^{a}	5.59 ± 0.34^{a}	5.25 ± 0.15^{a}	5.38 ± 0.09^{a}
TFC (mgRE/g DW)	18.47 ± 0.92^{a}	17.82 ± 1.75^{ab}	15.59 ± 0.61^{b}	15.12 ± 2.04^{b}
DPPH (%)	53.20 ± 0.95^{a}	52.61 ± 1.90^{ab}	50.19 ± 1.39^{bc}	48.23 ± 0.87^{c}
ABTS (%)	78.71 ± 0.37^{a}	79.22 ± 0.80^{a}	78.34 ± 0.85^{a}	78.29 ± 0.74^{a}

Note: DWGP represents the 6, 8, 10 and 12 d of wheatgrass powder; TPC, Total phenolic content; TFC, Total flavonoid content; DPPH, 2,2-diphenyl-1-picrylhydrazyl radical scavenging activity; ABTS, 2,2-azino-bis (3-ethylbenzothiazoline-6-sulphonic acid) radical scavenging activity. Different lowercase letters in the same rows indicate significant differences in germination days ($p < 0.05$).

3.2. Characteristics of steamed bread

The representative top-view and cross-section images of steamed bread incorporated by 2.5 % and 5 % addition levels of WGP are shown in Fig. 2 A. As compared to the control, the incorporation of WGP at a 2.5 % level significantly reduced the loaf volume of steamed bread by 23.63 %, 15.75 %, 17.80 %, and 16.43 % on 6, 8, 10, and 12 d, respectively. The higher level of WGP led to a further reduction in the loaf volume by 25.68 %, 26.02 %, 35.27 %, and 29.45 % with the increased germination days (Fig. 2 B). Incorporating WGP at 2.5 % and 5 % addition levels significantly increased the spread ratio of the steamed bread compared to the control (Fig. 2 C). Moreover, the steamed bread made by 8 d WGP at 2.5 % showed higher loaf volume and lower chewiness as compared to others. The firmness and chewiness of the steamed bread were increased by incorporating WGP, which might be due to the interaction of protein and dietary fiber within the gluten network. However, minor variations were seen in other texture properties (Fig. 2 D—H). Furthermore, including WGP decreased the L* and a* values of the steamed bread crust and crumb, while the b* value increased significantly (Table S1). This indicated that the lightness of the steamed bread decreased, and the color shifted towards yellow-green.

The taste and flavors of food products also play a crucial role in consumer acceptance and satisfaction (Ghasemi-Varnamkhasti et al., 2018). The sensory spider plots of the average responding values of 10 e-nose sensors to flavor compounds of each steamed bread sample are represented in Fig. 3 A-D. The response intensities of e-nose sensors W5S, W1S, W1W, W2S, and W2W were higher across all steamed bread samples, with minor fluctuations observed with 2.5 % to 5 % WGP addition. This suggested higher levels of nitrogen oxides, sulfur, ethanol, and certain aromatic compounds in samples exhibiting greater sensor sensitivity. The sensory spider plots of the average responding values of 10 e-tongue sensors to taste compounds of each steamed bread sample are represented in Fig. 3 *E*-H. The differences observed between different samples were sourness, where the addition of WGP potentially mitigates the sour taste in the steamed bread samples compared to the control, depending on the amount of WGP added. The incorporation of WGP into the steamed bread formulation potentially enriches and modifies its flavor and taste profile. This enhancement can be attributed to the bioactive compounds and phytochemicals present in wheat seedlings, which may interact with the bread matrix, leading to a distinctive sensory experience.

Based on the above results, wheatgrass germinated for 8 d and

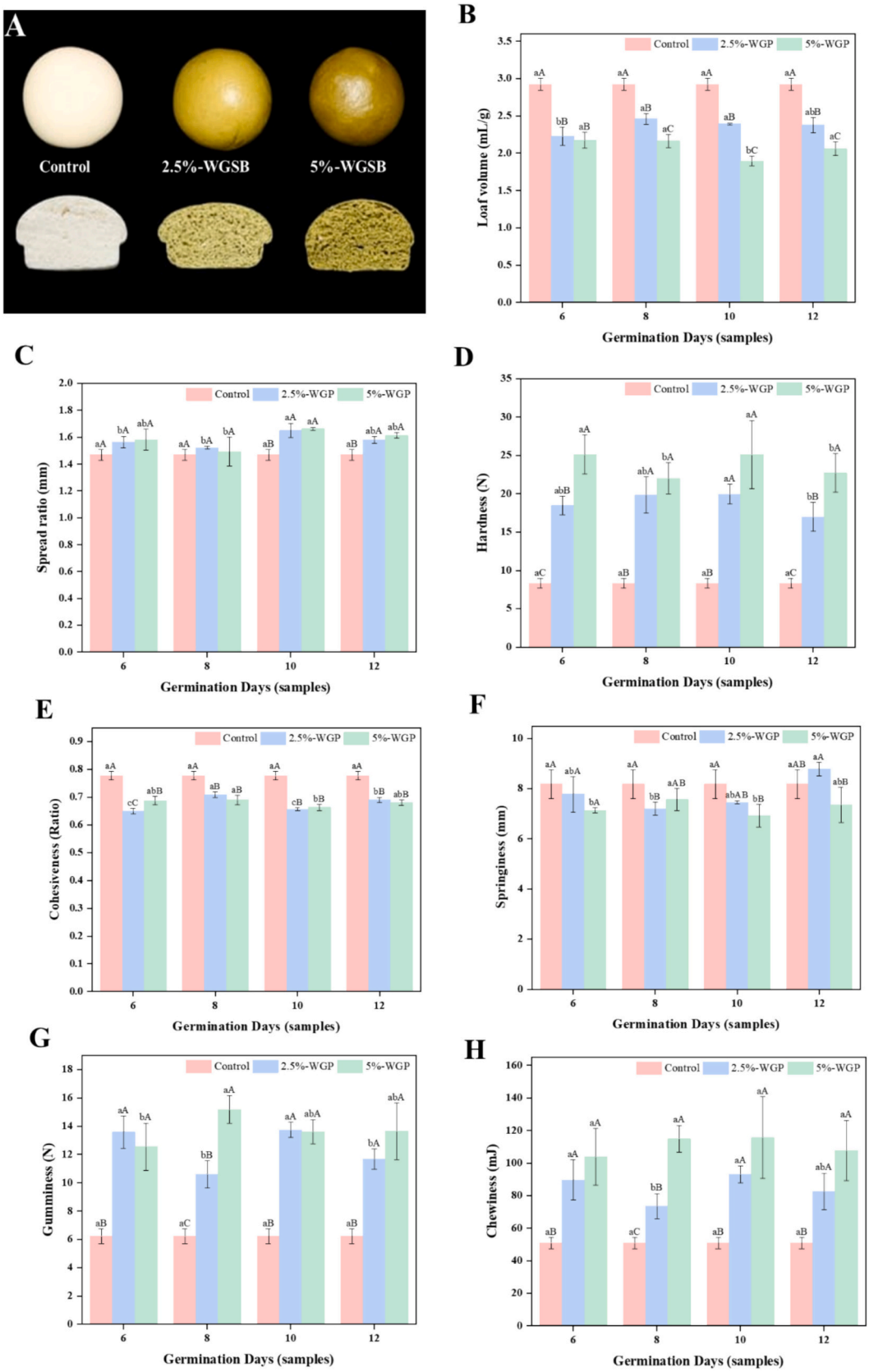

Fig. 2. The representative whole and cross-section images of steamed bread fortified with wheatgrass powder (2 A). The loaf volume (2 B), spread ratio (2C), and textural (hardness, cohesiveness, springiness, gumminess, and chewiness) parameters (2 D—H) of steamed bread made by the 6, 8, 10, and 12 d of wheatgrass powder. Where, control refers to steamed bread made without wheatgrass powder addition, 2.5 %-WGSB refers to steamed bread enriched with 2.5 %-wheatgrass powder, and 5 %-WGSB refers to steamed bread enriched with 5 %-wheatgrass powder. Different lowercase and capital letters indicate significant differences in the number of germination days at the same dosage level and in the same germination day at various dosage levels, respectively ($p < 0.05$).

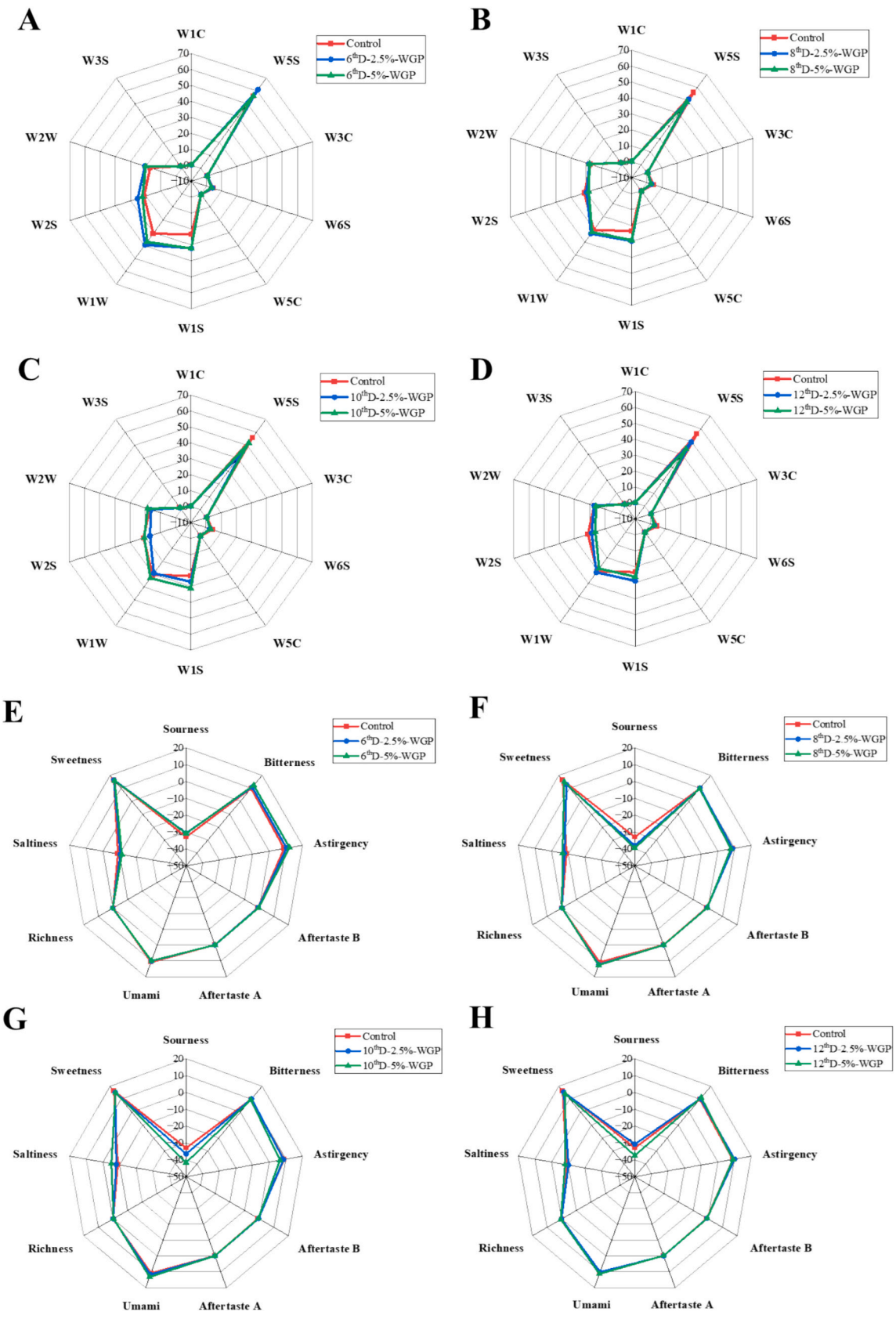

Fig. 3. Spider plots depicting sensory data obtained with the electronic nose (3 A-D) and with the electronic tongue (3 *E*-H) from steamed bread samples made by the 6, 8, 10 and 12 d of wheatgrass powder, Where Control refers to the steamed bread made without wheatgrass powder addition, 2.5 %-WGP refers as steamed bread enriched with 2.5 %-wheatgrass powder, 5 %-WGP refers as steamed bread enriched with 5 %-wheatgrass powder.

supplemented at 2.5 % dosage demonstrated the optimal nutritional and techno-functionality, and can be used as the functional ingredient for steamed bread. Therefore, the impact on the key components of dough, including the starch and gluten was further analyzed to demonstrate the underlying potential mechanism.

3.3. Pasting and gelation properties

The inclusion of WGP produced notable alterations in the pasting properties of the composite flours. The flour enriched with WGP significantly increased the peak viscosity (PV), breakdown viscosity (BV), while the trough viscosity (TV), setback viscosity (SV), and final viscosity (FV) were reduced (Fig. 4 A and Table S2). With the addition of WGP, the PV initially displayed an upward trend at a 2.5 % level, followed by a decline at a 5 % level. This might be due to the low level of WGP promoting the pasting of the starch, leading to the increased viscosity. However, as the percentage of WGP increased, the diluted concentration of starch was responsible for the decreased PV (Bawa et al., 2022). BV represents the disparity between PV and TV, primarily indicative of the resilience of starch granules when subjected to thermal and mechanical stress. The BV values of the composite flour with 2.5 % and 5 % WGP were markedly greater compared to the of regular wheat flour, indicating that the stability of starch granules in the composite flour was less thermal stable. This might be attributed to a weakened three-dimensional network of starch gels with WGP, thereby reducing the thermal stability. Furthermore, the FV reflects the re-association of starch granules during cooling, indicating the stability throughout the heating-cooling cycle (Panghal et al., 2019; Kaur et al., 2021). The addition of WGP reduced both FV and SV of the wheat flour, likely because the WGP could delay the retrogradation and rearrangement of starch by tightly connecting with the starch molecules, which was beneficial for the preservation of wheat-derived products (Bawa et al., 2022).

3.4. Molecular weight (Mw) distribution and free sulfhydryl (SH) content of gluten protein

During dough processing, gluten proteins undergo reactions of polymerization and depolymerization, which result from the formation and cleavage of chemical bonds between protein molecules. This dynamic interaction leads to changes in the molecular weight (Mw) of the gluten proteins. The SDS-soluble protein (SDS-P) content is crucial in assessing the extent of protein cross-linking. The area corresponding to the polymer peak (SDS-P) predominantly comprises glutenin polymers, with Mw ranging from approximately 91,000 to 688,000 Da. In contrast, the monomer peak (SDS-M) area includes monomeric glutenin, gliadins with Mw between approximately 2000 and 91,000 Da, and smaller peptides and amino acids with Mw below 2000 Da. The SDS-insoluble fraction (SDS-I), which is characterized as the glutenin macromolecular polymer (GMP), represents the high-molecular-weight glutenin polymer network in the unheated dough. Upon heating, this fraction undergoes structural modifications, forming glutenin-gliadin macrocrosslinks, which are integral to the dough's cohesiveness and elasticity. Representative chromatograms of the SDS-soluble proteins are shown in Fig. 4 B. Throughout the fermentation process, the levels of SDS-P and SDS-M either remained stable or decreased slightly, reflecting the ongoing protein interactions and modifications. However, a more significant reduction in these fractions was observed following steaming (Table 2). This reduction correlates with structural transitions in the gluten proteins, including unfolding, dissociation, and re-aggregation, which occur during the thermal processing of the dough into steamed bread. These transitions influence the dough's final texture, consistency, and other techno-functional properties. The reduction in SDS-P and SDS-M levels during the steaming process was the primary reason for the increase in SDS-I. This phenomenon can be ascribed to the aggregation of gliadins and glutenins induced by heat, which facilitates the formation of intermolecular disulfide (SS) bonds (Tang et al., 2017; Zhang et al., 2024). Meanwhile, the elevated levels of SDS-M in the WGP enriched samples during the mixing and fermentation stages might be associated with the activated proteases in wheatgrass. The synergistic hydrolysis of insoluble proteins by proteases and yeast led to an increase in soluble protein content. Furthermore, compared to the control, the inclusion of WGP resulted in a lower SDS-I level in the steamed bread, likely due to dietary fiber interfering with the gluten network and hindering heat-induced aggregation (Bawa et al., 2022; Zhou et al., 2021). Notably, steamed bread with a high content of WGP exhibited a lower SDS-I level, indicating that increasing the dosage could enhance the inhibitory effect of WGP on the cross-linking reaction.

The free SH content is an indicator for assessing the fluctuations in the formation of SS bonds that promote glutenin and gliadin aggregation and the development of the gluten network (Wieser et al., 2023). The content of the SH was highest prior to steaming, suggesting that the gluten protein structure was least compacted during the mixing and fermentation stages. The reduction in the SH content after steaming can be attributed to glutenin-gliadin aggregation, which was in accordance with the results of the increased SDS-I (Zhao et al., 2020). Besides, the incorporation of WGP at all stages notably increased the SH content, particularly during the steaming stage, compared with the control group. This might be due to the participation of dietary fiber, which reduced the compactness of the gluten protein structure. Additionally, during the heating phase, both the oxidation of SH groups to SS bonds and the exchange mechanism between SH groups and SS bonds occurred simultaneously (Wang, Liu, et al., 2019). This reaction had a negligible impact on the concentration of free SH groups, leading to a high level of SH content in samples with the incorporation of WGP. Furthermore, the findings indicated that the content of SH and SDS-M increased with a higher amount of WGP, while the content of SDS-I decreased correspondingly. This indicated that the presence of WGP could inhibit the polymerization of gluten during the steaming process. The heat-induced aggregation of glutenins and gliadins plays a crucial role in forming the structural network, significantly influencing the product's volume and texture. This may account for the notable reduction in the quality of the steamed bread, as the degree of crosslinking between glutenins and gliadins has been shown to be favorably connected with the degraded product quality (Wang et al., 2015).

3.5. Distribution of different protein subunits

The alternations in different protein subunits, including gliadin and glutenin, during the processing process of steamed bread were analyzed using RP-HPLC (Fig. 4 C and D), and the quantitative testing results are presented in Table 3. These changes reflect the complex interactions of gluten proteins during bread making. After steaming, a reduction in gliadin subunits and an acceleration in glutenin subunits were observed, suggesting that the gliadin subunits became insoluble and involved in protein aggregation during the steaming process (Wang, Hou, et al., 2019; Wang, Liu, et al., 2019). The α- and γ-gliadins exhibited significant reduction following the steaming process. In contrast, there was a corresponding increase in the high molecular weight glutenin subunit (HMS) and low molecular weight glutenin subunit (LMS). This observation aligns with previous studies on wheat-based products, where heat treatment led to substantial protein aggregates and decreased monomeric proteins (Zhang et al., 2007). Compared to the control, WGP enhanced the proportion of α- and γ-gliadins and diminished the proportion of HMS and LMS in steamed bread, also suggesting that WGP could reduce the degree and rate of heat-induced polymerization of gluten. The outcomes were consistent with the Mw and SH content of gluten proteins. Similarly, besides dietary fiber, the polyphenolic compounds present in WGP could also modulate gluten aggregation. Polyphenols have been reported to form complexes with gluten proteins, potentially inhibiting the aggregation process (Girard & Awika, 2020). The proteases in WGP could also partially hydrolyze gluten proteins,

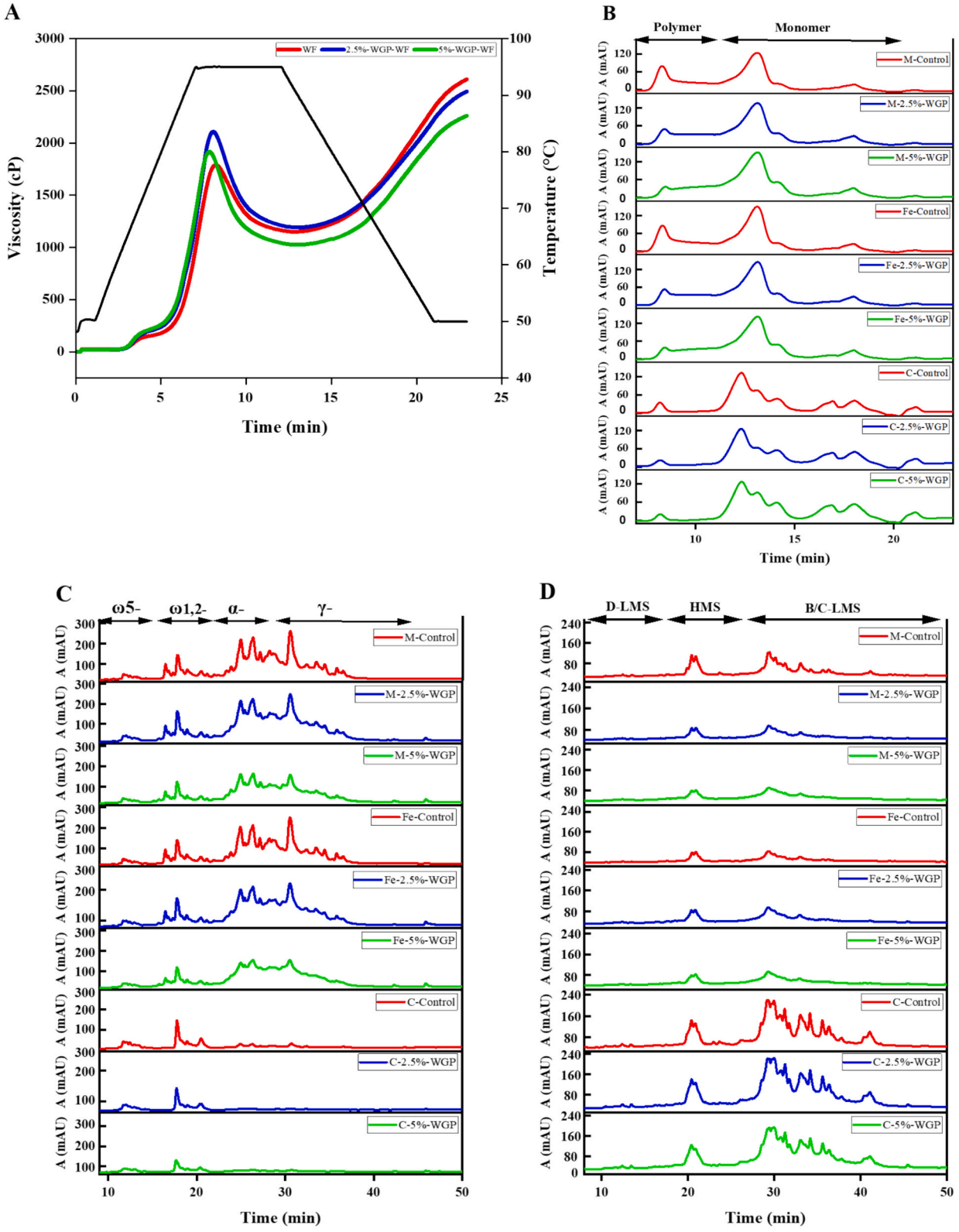

Fig. 4. RVA curves of common wheat flour and flour enriched with wheatgrass powder (4 A); Where WF refers to wheat flour, 2.5 %-WGP-WF refers to wheat flour enriched with 2.5 %-wheatgrass powder, 5 %-WGP-WF refers to wheat flour enriched with 5 %-wheatgrass powder. Typical non-reduced SE-HPLC curves (4 B) during the steamed bread-making process; Typical RP-HPLC curves of ethanol soluble (4C) and insoluble (4 D) proteins during the steamed bread-making process; Where M-control refers to a mixed dough control sample, M-2.5 %-WGP refers to mixed dough containing 2.5 % wheatgrass powder, M-5 %-WGP refers to mixed dough containing 5 % wheatgrass powder; Fe-control refers to fermented dough control sample, Fe-2.5 %-WGP refers to fermented dough containing 2.5 % wheatgrass powder, Fe-5 %-WGP refers to fermented dough containing 5 % wheatgrass powder; C-control refers to crumb of steamed bread control sample, C-2.5 %-WGP refers to crumb of steamed bread containing 2.5 % wheatgrass powder, C-5 %-WGP refers to crumb of steamed bread containing 5 % wheatgrass powder.

Table 2
Changes in molecular weight (Mw) distribution of proteins and SH content during the processing stages of steamed bread.

Samples	Processing stages	Mw distribution of gluten (%)			SH content (μmol/g)
		SDS-P	SDS-M	SDS-I	
Control	Mixed dough	8.57 ± 0.52^{aB}	17.14 ± 1.38^{cA}	74.29 ± 0.95^{bB}	6.29 ± 0.26^{cA}
2.5 %-WGP		1.75 ± 0.32^{bA}	19.75 ± 1.55^{bA}	78.49 ± 1.86^{aB}	7.36 ± 0.12^{bA}
5 %-WGP		0.92 ± 0.07^{cB}	26.20 ± 2.07^{aA}	72.88 ± 2.08^{bC}	9.63 ± 0.15^{aA}
Control	Fermented dough	8.81 ± 1.06^{aA}	16.60 ± 2.22^{bB}	74.59 ± 1.16^{bB}	5.55 ± 0.06^{cB}
2.5 %-WGP		2.19 ± 0.10^{bA}	17.88 ± 1.68^{bB}	79.92 ± 1.62^{aB}	6.76 ± 0.15^{bB}
5 %-WGP		1.06 ± 0.09^{cA}	24.50 ± 1.59^{aB}	74.44 ± 1.68^{bB}	8.32 ± 0.14^{aB}
Control	Steamed bread	0.53 ± 0.08^{bC}	3.93 ± 0.83^{bC}	95.54 ± 0.99^{aA}	3.54 ± 0.09^{cC}
2.5 %-WGP		0.71 ± 0.12^{abB}	4.71 ± 1.22^{abC}	94.58 ± 2.10^{abA}	4.88 ± 0.22^{bC}
5 %-WGP		0.79 ± 0.09^{aC}	5.52 ± 1.34^{aC}	93.69 ± 1.24^{bA}	7.21 ± 0.10^{aC}

Note: Control refers to sample without WGP addition, 2.5 %-WGP refers to sample enriched with 2.5 %-wheat grass powder, and 5 %-WGP refers to sample enriched with 5 %-wheat grass powder. SDS-P, SDS soluble polymers; SDS-M, SDS soluble monomers; SDS-I, insoluble proteins; SH, sulfhydryl content. Different lowercase and capital letters indicate significant differences between the samples under the same processing stage and the samples under different processing stages, respectively ($p < 0.05$).

Table 3
Protein subunit distribution during the processing stages of steamed bread.

Samples	Processing stages	ω5-gliadin	ω1,2-gliadin	α-gliadin	γ-gliadin	D-LMS	HMS	B/C-LMS
Control	Mixed dough	2.20 ± 0.21^{bB}	11.81 ± 0.60^{aA}	38.14 ± 0.84^{aA}	20.14 ± 0.42^{aA}	1.32 ± 0.05^{cC}	4.14 ± 0.45^{bC}	13.82 ± 0.96^{abB}
2.5 %-WGP		2.24 ± 0.03^{abC}	11.13 ± 0.14^{aA}	35.28 ± 0.32^{bA}	18.17 ± 0.39^{bA}	1.59 ± 0.04^{bB}	4.57 ± 0.55^{bB}	13.66 ± 0.38^{bB}
5 %-WGP		2.52 ± 0.14^{aB}	11.40 ± 0.05^{aA}	34.14 ± 0.28^{cA}	17.65 ± 0.92^{bA}	1.88 ± 0.06^{aB}	5.46 ± 0.38^{aB}	15.06 ± 0.57^{aB}
Control	Fermented dough	2.37 ± 0.05^{bAB}	11.98 ± 0.03^{aA}	35.95 ± 0.54^{aB}	18.75 ± 0.68^{aB}	1.49 ± 0.02^{cB}	4.79 ± 0.56^{bB}	12.31 ± 1.10^{cC}
2.5 %-WGP		2.64 ± 0.07^{aB}	11.69 ± 0.13^{aA}	34.07 ± 0.63^{bB}	17.15 ± 0.75^{bB}	1.62 ± 0.06^{bB}	4.81 ± 0.23^{bB}	13.06 ± 1.00^{bB}
5 %-WGP		2.43 ± 0.19^{abB}	11.12 ± 0.27^{bB}	32.25 ± 1.06^{cB}	16.33 ± 0.45^{bB}	1.92 ± 0.02^{aB}	5.61 ± 0.35^{aB}	15.00 ± 0.43^{aB}
Control	Steamed bread	2.64 ± 0.15^{bA}	6.27 ± 0.07^{bB}	2.90 ± 0.10^{cC}	1.72 ± 0.14^{bC}	2.52 ± 0.11^{aA}	31.27 ± 0.42^{aA}	50.56 ± 0.28^{aA}
2.5 %-WGP		2.89 ± 0.16^{abA}	6.35 ± 0.04^{bB}	3.32 ± 0.08^{bC}	1.79 ± 0.12^{aC}	2.28 ± 0.07^{bA}	28.26 ± 0.68^{bA}	49.53 ± 0.46^{aA}
5 %-WGP		3.13 ± 0.13^{aA}	6.59 ± 0.17^{aC}	3.58 ± 0.12^{aC}	1.82 ± 0.08^{aC}	2.09 ± 0.05^{cA}	26.25 ± 0.76^{cA}	47.40 ± 0.88^{bA}

Note: Different lowercase and capital letters indicate significant differences between the samples under the same processing stage and the samples under different processing stages, respectively ($p < 0.05$).

resulting in smaller peptides that were less likely to participate in extensive heat-induced aggregation that might contribute to the observed relative increase in α- and γ-gliadins subunits in WGP-enriched samples by affecting the gluten polymerization. In contrast, marginal changes were observed in the ω-gliadin subunits. This was because the α- and γ-gliadins involved in the macromolecular glutenin-gliadin network via heat-induced covalent cross-linking were found to be extractable following reduction with DTT. This extraction process was further reflected in the RP-HPLC profiles of the HMS and D-LMS fractions (Wang, Liu, et al., 2019).

3.6. Microstructure of dough

Scanning electron microscopy (SEM) was employed to observe the microstructural impact of WGP on the gluten network and starch granules in steamed bread dough. The control sample (without WGP) exhibited a well-organized gluten matrix, where starch granules were uniformly encapsulated within a continuous, cohesive gluten network (Fig. 5 A). With the addition of 2.5 % WGP, the gluten network displayed signs of disintegration, with partial exposure of starch granules and the appearance of voids within the gluten structure (Fig. 5 B). The gluten matrix became less compact, indicating early signs of weakened gluten-starch interactions. At 5 % WGP, these structural disruptions became more pronounced, that may reveal a denser structure with fewer and smaller air pockets or voids (Fig. 5 C). This could correspond to the increase in firmness and chewiness of the steamed bread, as observed in the quality parameters. The gluten network became discontinuous and heterogeneous, with larger gaps between gluten strands and increased exposure to starch granules. Many starch granules remained ungelatinized, retaining their granular form. This suggests that WGP inhibited starch gelatinization, likely by interfering with the water-gluten interaction required for network formation. The disruption of

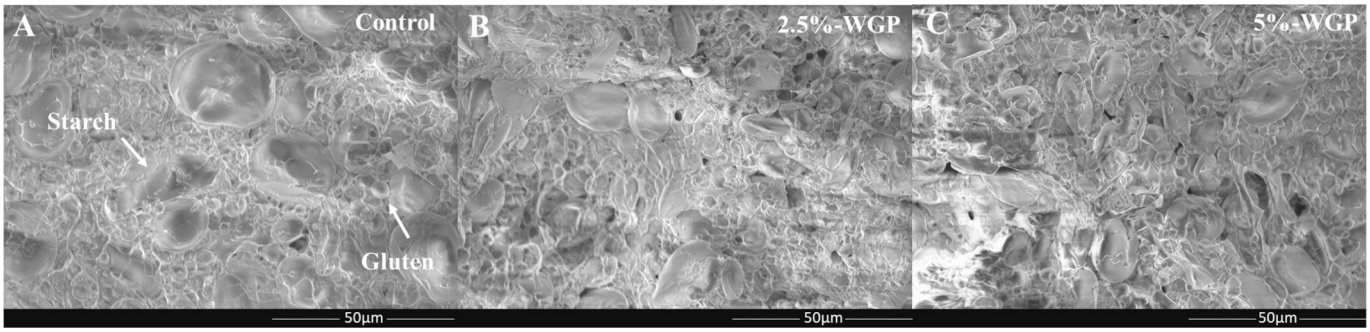

Fig. 5. The SEM images of the microstructure of the dough samples, Control (5 A), 2.5 %-WGP (5 B), 5 %-WGP (5C); Control refers to the dough sample made without wheatgrass powder addition, 2.5 %-WGP refers to dough sample enriched with 2.5 %-wheatgrass powder, 5 %-WGP refers as dough sample enriched with 5 %-wheatgrass powder.

the gluten network and reduced starch encapsulation could be due to competition for water between the WGP components (fiber and protein) and gluten, resulting in insufficient gluten hydration (Bawa et al., 2022; Rahman et al., 2015). These results suggest that the inclusion of WGP at higher concentrations significantly alters the gluten-starch matrix in steamed bread, implying the need for formulation adjustments to maintain optimal dough properties.

4. Conclusion

In this study, germinated wheat seedlings harvested at 8 days were considered an optimal source for enriching steamed bread through a comprehensive analysis of bioactive compounds and steamed bread quality parameters. The incorporation of WGP reduced loaf volume while increasing the firmness and chewiness of the bread, alongside imparting a distinctive yellow-greenish color, which could enhance consumer appeal. WGP also improved the flavor and taste profiles. Furthermore, it inhibited starch gelatinization and reduced thermal stability while modulating the polymerization of gluten proteins, specifically suppressing the heat-induced polymerization of α- and γ-gliadin into glutenin. SEM analysis revealed that WGP disrupted the gluten-starch network, leading to structural fragmentation and decreased starch gelatinization, which contributed to the observed textural changes. Overall, this research offers valuable insights into the functional and nutritional enhancement of steamed bread using plant-based ingredients and highlights the potential for further studies on improving food quality and safety through such additives.

CRediT authorship contribution statement

Muhammad Bilal: Writing – original draft, Methodology, Data curation, Conceptualization. **Yiwei Wu:** Software, Data curation. **Guangzheng Wang:** Visualization, Data curation. **Guannan Liu:** Validation, Investigation. **Muhammad Shahar Yar:** Validation, Software. **Dandan Li:** Writing – review & editing. **Chong Xie:** Writing – review & editing. **Runqiang Yang:** Writing – review & editing. **Dong Jiang:** Resources, Project administration. **Pei Wang:** Writing – review & editing, Supervision, Funding acquisition, Conceptualization.

Declaration of competing interest

The authors declare that they have no known competing financial interests or personal relationships that could have appeared to influence the work reported in this paper.

Acknowledgments

This research was supported by the Hainan Province Science and Technology Special Fund (ZDYF2022XDNY233), the Fundamental Research Funds for the Central Universities (KJYQ2024022), National key research and development plan project (2022YFD2301401), Young Elite Scientists Sponsorship Program by the CAST (2022QNRC001), the Central Government Guides Local Funds (ZYYD2023A13), and a project funded by the Priority Academic Program Development (PAPD) of Jiangsu Higher Education Institutions.

Appendix A. Supplementary data

Supplementary data to this article can be found online at https://doi.org/10.1016/j.fochx.2025.102306.

Data availability

Data will be made available on request.

References

AACC International (2000). Approved methods of the American Association of Cereal Chemists. Methods 44–16.01, 39-25.01, 58-19.01, 08-01.01, 32-05.01.

Bawa, K., Brar, J. K., Singh, A., Gupta, A., Kaur, H., & Bains, K. (2022). Wheatgrass powder-enriched functional pasta: Techno-functional, phytochemical, textural, sensory, and structural characterization. *Journal of Texture Studies, 53*(4), 517–530. https://doi.org/10.1111/jtxs.12680

Beveridge, T., Toma, S. J., & Nakai, S. (1974). Determination of SH-and SS-groups in some food proteins using Ellman's reagent. *Journal of Food Science, 39*, 49–51. https://doi.org/10.1111/j.1365-2621.1974.tb00984.x

Bilal, M., Li, D., Xie, C., Yang, R., Gu, Z., Jiang, D., Xu, X., & Wang, P. (2024). Recent advances of wheat bran arabinoxylan exploitation as the functional dough additive. *Food Chemistry, 141146*. https://doi.org/10.1016/j.foodchem.2024.141146

Bilal, M., Zhang, Y., Li, D., Xie, C., Yang, R., Gu, Z., Jiang, D., & Wang, P. (2023). Optimizing techno-functionality of germinated whole wheat flour steamed bread via glucose oxidase (Gox) and pentosanase (Pn) enzyme innovation. *Grain & Oil Science and Technology, 6*(4), 219–226. https://doi.org/10.1016/j.gaost.2023.11.002

Devi, C. B., Bains, K., & Kaur, H. (2019). Effect of drying procedures on nutritional composition, bioactive compounds and antioxidant activity of wheatgrass (*Triticum aestivum* L). *Journal of Food Science and Technology, 56*, 491–496. https://doi.org/10.1007/s13197-018-3473-7

Dudonne, S., Vitrac, X., Coutiere, P., Woillez, M., & Mérillon, J. M. (2009). Comparative study of antioxidant properties and total phenolic content of 30 plant extracts of industrial interest using DPPH, ABTS, FRAP, SOD, and ORAC assays. *Journal of Agricultural and Food Chemistry, 57*(5), 1768–1774. https://doi.org/10.1021/jf803011r

Ghasemi-Varnamkhasti, M., Apetrei, C., Lozano, J., & Anyogu, A. (2018). Potential use of electronic noses, electronic tongues and biosensors as multisensor systems for spoilage examination in foods. *Trends in Food Science & Technology, 80*, 71–92. https://doi.org/10.1016/j.tifs.2018.07.018

Ghumman, A., Singh, N., & Kaur, A. (2017). Chemical, nutritional and phenolic composition of wheatgrass and pulse shoots. *International Journal of Food Science & Technology, 52*(10), 2191–2200. https://doi.org/10.1111/ijfs.13498

Girard, A. L., & Awika, J. M. (2020). Effects of edible plant polyphenols on gluten protein functionality and potential applications of polyphenol–gluten interactions. *Comprehensive Reviews in Food Science and Food Safety, 19*(4), 2164–2199. https://doi.org/10.1111/1541-4337.12572

Hiscox, J. D., & Israelstam, G. F. (1979). A method for the extraction of chlorophyll from leaf tissue without maceration. *Canadian Journal of Botany, 57*(12), 1332–1334. https://doi.org/10.1139/b79-163

Huang, S., Betker, S., Quail, K., & Moss, R. (1993). An optimized processing procedure by response surface methodology (RSM) for northern-style Chinese steamed bread. *Journal of Cereal Science, 18*(1), 89–102. https://doi.org/10.1006/jcrs.1993.1037

Kaur, N., Singh, B., Kaur, A., Yadav, M. P., Singh, N., Ahlawat, A. K., & Singh, A. M. (2021). Effect of growing conditions on proximate, mineral, amino acid, phenolic composition and antioxidant properties of wheatgrass from different wheat (*Triticum aestivum L.*) varieties. *Food Chemistry, 341*, Article 128201. https://doi.org/10.1016/j.foodchem.2020.128201

Lee, W. D., Pirona, A. C., Sarvin, B., Stern, A., Nevo-Dinur, K., Besser, E., … Shlomi, T. (2021). Tumor reliance on cytosolic versus mitochondrial one-carbon flux depends on folate availability. *Cell Metabolism, 33*(1), 190–198. https://doi.org/10.1016/j.cmet.2020.12.002

Li, S., Liu, F., Wu, M., Li, Y., Song, X., & Yin, J. (2023). Effects of drying treatments on nutritional compositions, volatile flavor compounds, and bioactive substances of broad beans. *Foods, 12*(11), 2160. https://doi.org/10.3390/foods12112160

Li, W., Cao, W., Wang, P., Li, J., Zhang, Q., & Yan, Y. (2021). Selectively hydrolyzed soy protein as an efficient quality improver for steamed bread and its influence on dough components. *Food Chemistry, 359*, Article 129926. https://doi.org/10.1016/j.foodchem.2021.129926

Liu, F., Xiang, N., Hu, J. G., Shijuan, Y., Xie, L., Brennan, C. S., … Guo, X. (2017). The manipulation of gene expression and the biosynthesis of vitamin C, E and folate in light-and dark-germination of sweet corn seeds. *Scientific Reports, 7*(1), 7484. https://doi.org/10.1038/s41598-017-07774-9

Liu, G., Zhou, J., Wu, S., Fang, S., Bilal, M., Xie, C., Wang, P., Yin, Y., & Yang, R. (2024). Novel strategy to raise the content of aglycone isoflavones in soymilk and gel: Effect of germination on the physicochemical properties. *Food Research International, 186*, Article 114335. https://doi.org/10.1016/j.foodres.2024.114335

Liu, W., Fan, Y., Liu, Q., Xu, F., Zhang, L., & Hu, H. (2023). Identification of the flavor profiles of Chinese pancakes from various areas using smart instruments combined with E-noses and E-tongues. *International Journal of Agricultural and Biological Engineering, 16*(1), 283–290. https://doi.org/10.25165/j.ijabe.20231601.6817

Ma, M., Wang, P., Yang, R., & Gu, Z. (2018). Effects of UV-B radiation on the isoflavone accumulation and physiological-biochemical changes of soybean during germination: Physiological-biochemical change of germinated soybean induced by UV-B. *Food Chemistry, 250*, 259–267. https://doi.org/10.1016/j.foodchem.2018.01.051

Nonogaki, H., Bassel, G. W., & Bewley, J. D. (2010). Germination—Still a mystery. *Plant Science, 179*(6), 574–581. https://doi.org/10.1016/j.plantsci.2010.02.010

Panghal, A., Kaur, R., Janghu, S., Sharma, P., Sharma, P., & Chhikara, N. (2019). Nutritional, phytochemical, functional and sensorial attributes of *Syzygium cumini* L. pulp incorporated pasta. *Food Chemistry, 289*, 723–728. https://doi.org/10.1016/j.foodchem.2019.03.081

Parenti, O., Guerrini, L., & Zanoni, B. (2020). Techniques and technologies for the breadmaking process with unrefined wheat flours. *Trends in Food Science & Technology, 99*, 152–166. https://doi.org/10.1016/j.tifs.2020.02.034

Rahman, R., Hiregoudar, S., Veeranagouda, M., Ramachandra, C. T., Nidoni, U., Roopa, R. S., Kowalski, R. J., & Ganjyal, G. M. (2015). Effects of wheat grass powder incorporation on physiochemical properties of muffins. *International Journal of Food Properties, 18*(4), 785–795. https://doi.org/10.1080/10942912.2014.908389

Riaz, B., Liang, Q., Wan, X., Wang, K., Zhang, C., & Ye, X. (2019). Folate content analysis of wheat cultivars developed in the North China plain. *Food Chemistry, 289*, 377–383. https://doi.org/10.1016/j.foodchem.2019.03.028

Sani, I. K., Mehrnoosh, F., Rasul, N. H., Hassani, B., Mohammadi, H., Gholizadeh, H., & Jafari, S. M. (2024). Pulsed electric field-assisted extraction of natural colorants; principles and applications. *Food Bioscience, 104746*. https://doi.org/10.1016/j.fbio.2024.104746

Tang, K. X., Zhao, C. J., & Gänzle, M. G. (2017). Effect of glutathione on the taste and texture of type I sourdough bread. *Journal of Agricultural and Food Chemistry, 65*(21), 4321–4328. https://doi.org/10.1021/acs.jafc.7b00897

Wang, G., Qu, X., Li, D., Yang, R., Gu, Z., Jiang, D., & Wang, P. (2023). Enhancing the technofunctionality of γ-aminobutyric acid enriched germinated wheat by modification of arabinoxylan, gluten proteins and liquid lamella of dough. *Food Chemistry, 404*, Article 134523. https://doi.org/10.1016/j.foodchem.2022.134523

Wang, P., Hou, C., Zhao, X., Tian, M., Gu, Z., & Yang, R. (2019). Molecular characterization of water-extractable arabinoxylan from wheat bran and its effect on the heat-induced polymerization of gluten and steamed bread quality. *Food Hydrocolloids, 87*, 570–581. https://doi.org/10.1016/j.foodhyd.2018.08.049

Wang, P., Liu, K., Yang, R., Gu, Z., Zhou, Q., & Jiang, D. (2019). Comparative study on the bread making quality of normoxia-and hypoxia-germinated wheat: Evolution of γ-aminobutyric acid, starch gelatinization, and gluten polymerization during steamed bread making. *Journal of Agricultural and Food Chemistry, 67*(12), 3480–3490. https://doi.org/10.1021/acs.jafc.9b00200

Wang, P., Tao, H., Jin, Z., & Xu, X. (2015). The final established physicochemical properties of steamed bread made from frozen dough: Study of the combined effects of gluten polymerization, water content and starch crystallinity on bread firmness. *Journal of Cereal Science, 63*, 116–121. https://doi.org/10.1016/j.jcs.2015.03.008

Wang, P., Zou, M., Gu, Z., & Yang, R. (2018). Heat-induced polymerization behavior variation of frozen-stored gluten. *Food Chemistry, 255*, 242–251. https://doi.org/10.1016/j.foodchem.2018.02.047

Wang, Z., Ma, S., Sun, B., Wang, F., Huang, J., Wang, X., & Bao, Q. (2021). Effects of thermal properties and behavior of wheat starch and gluten on their interaction: A review. *International Journal of Biological Macromolecules, 177*, 474–484. https://doi.org/10.1016/j.ijbiomac.2021.02.175

Wieser, H., Koehler, P., & Scherf, K. A. (2023). Chemistry of wheat gluten proteins: Qualitative composition. *Cereal Chemistry, 100*(1), 23–35. https://doi.org/10.1002/cche.10572

Xu, L., Wang, P., Ali, B., Yang, N., Chen, Y., Wu, F., & Xu, X. (2017). Changes of the phenolic compounds and antioxidant activities in germinated adlay seeds. *Journal of the Science of Food and Agriculture, 97*(12), 4227–4234. https://doi.org/10.1002/jsfa.8298

Zhang, P., He, Z., Chen, D., Zhang, Y., Larroque, O. R., & Xia, X. (2007). Contribution of common wheat protein fractions to dough properties and quality of northern-style Chinese steamed bread. *Journal of Cereal Science, 46*(1), 1–10. https://doi.org/10.1016/j.jcs.2006.10.007

Zhang, Y., Geng, Q., Song, M., Li, X., Yang, A., Tong, P., Wu, Z., & Chen, H. (2024). The structure and potential allergenicity of peanut allergen monomers after roasting. *Food & Function, 15*(5), 2577–2586. https://doi.org/10.1039/D3FO05351B

Zhao, X., Hou, C., Tian, M., Zhou, Y., Yang, R., Wang, X., Gu, Z., & Wang, P. (2020). Effect of water-extractable arabinoxylan with different molecular weight on the heat-induced aggregation behavior of gluten. *Food Hydrocolloids, 99*, Article 105318. https://doi.org/10.1016/j.foodhyd.2019.105318

Zhou, Y., Dhital, S., Zhao, C., Ye, F., Chen, J., & Zhao, G. (2021). Dietary fiber-gluten protein interaction in wheat flour dough: Analysis, consequences and proposed mechanisms. *Food Hydrocolloids, 111*, Article 106203. https://doi.org/10.1016/j.foodhyd.2020.106203